JCTC Journal of Chemical Theory and Computation

pubs.acs.org/JCTC Article

Roles of H-Bonding and Hydride Solvation in the Reaction of Hydrated (Di)electrons with Water to Create H_2 and OH^-

William R. Borrelli, José L. Guardado Sandoval, Kenneth J. Mei, and Benjamin J. Schwartz*

Cite This: J. Chem. Theory Comput. 2024, 20, 7337−7346 Read Online

ABSTRACT: Even though single hydrated electrons (e^-_{hyd}'s) are stable in liquid water, two hydrated electrons can bimolecularly react with water to create H_2 and hydroxide: $e^-_{hyd} + e^-_{hyd} + 2H_2O \rightarrow H_2 + 2OH^-$. The rate of this reaction has an unusual temperature and isotope dependence as well as no dependence on ionic strength, which suggests that cosolvation of two electrons as a single hydrated dielectron ($e^{2-}_{2,hyd}$) might be an important intermediate in the mechanism of this reaction. Here, we present an ab initio density functional theory study of this reaction to better understand the potential properties, reactivity, and experimental accessibility of hydrated dielectrons. Our simulations create hydrated dielectrons by first simulating single e^-_{hyd}'s and then injecting a second electron, providing a well-defined time zero for $e^{2-}_{2,hyd}$ formation and offering insight into a potential experimental route to creating dielectrons and optically inducing the reaction. We find that $e^{2-}_{2,hyd}$ immediately forms in every member of our ensemble of trajectories, allowing us to study the molecular mechanism of H_2 and OH^- formation. The subsequent reaction involves separate proton transfer steps with a generally well-defined hydride subintermediate. The time scales for both proton transfer steps are quite broad, with the first proton transfer step spanning times over a few ps, while the second proton transfer step varies over ∼150 fs. We find that the first proton transfer rate is dictated by whether or not the reacting water is part of an H-bond chain that allows the newly created OH^- to rapidly move by Grotthuss-type proton hopping to minimize electrostatic repulsion with H^-. The second proton transfer step depends significantly on the degree of solvation of H^-, leading to a wide range of reactive geometries where the two waters involved can lie either across the dielectron cavity or more adjacent to each other. This also allows the two proton transfer events to take place either effectively concertedly or sequentially, explaining differing views that have been presented in the literature.

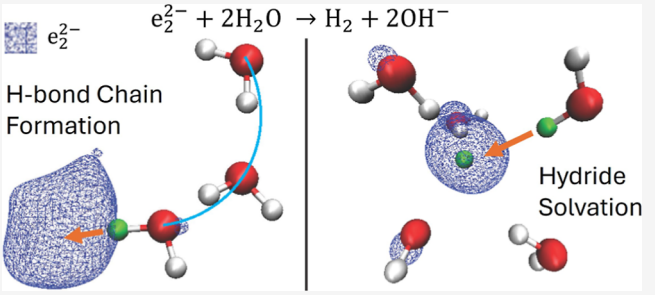

INTRODUCTION

When an excess electron is formed in liquid water, a stably solvated species known as the hydrated electron (e^-_{hyd}) is formed. Hydrated electrons have garnered significant theoretical and experimental interest due to their fascinating properties, reactivity, and pertinence to a variety of fields such as radiation chemistry,[1−4] biochemistry,[4,5] and atmospheric chemistry.[6] Though hydrated electrons have been extensively studied by both simulation[7−18] and experiment,[1−3,19−22] much remains unknown about the solvation structure of hydrated electrons[4,7,15−17,23−25] as well as about the mechanism of their reactivity as strong reducing agents in solution.[14,26−28]

One of the reasons that hydrated electrons are not a stable equilibrium species is that they not only react with protons in water (which are naturally present at 10^{-7} M concentration) but they also can react with each other. The latter process, which we refer to as the dielectron hydrogen evolution (DEHE) reaction,[16] can be summarized as[29]

$$e^-_{hyd} + e^-_{hyd} + 2H_2O \rightarrow H_2 + 2OH^- \quad (1)$$

The rate of this reaction is diffusion-limited and also independent of ionic strength.[30] The DEHE reaction has an unusual temperature dependence, with Arrhenius-like behavior up until 150 °C followed by a decrease in rate with increasing temperature and then plateauing of the rate at a higher temperatures.[3] There is also a significant isotopic enrichment factor that strongly favors H over D.[29,31] The absence of atomic hydrogen in the reaction products[31] suggests that H· is not an intermediate in the reaction process. The fact that triplet H_2 is not bound[30] means that whatever the reactive dielectron species is, the two electrons that react must be initially spin singlet.

Although the detailed mechanism of the DEHE reaction is not definitively known, the behaviors of the DEHE reaction described above imply that there likely is a reactive intermediate

Received: June 14, 2024
Revised: July 26, 2024
Accepted: July 29, 2024
Published: August 7, 2024

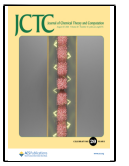

in which two hydrated electrons combine to form a hydrated dielectron ($e^{2-}_{2,hyd}$) prior to reacting.[1,3,32,33] Dielectrons should have more reducing power than single hydrated electrons and thus are likely better able to react with the surrounding water.[33] The idea that $e^{2-}_{2,hyd}$ might be a quasi-stable species has inspired a host of mixed quantum/classical[34−37] and ab initio[15,38] simulations to learn about the properties of this possible reactive intermediate. Recent experimental work from Hartweg et al.[39] has shown indirect evidence of dielectrons forming in ammonia solutions. Of particular interest is what the solvation structure of dielectrons might be: do the two paired electrons occupy a single cavity in solution, or are they instead solvated in separate but nearby cavities and exist as a solvent-separated pair?[29]

Whether or not dielectrons are involved in the DEHE reaction, two groups have performed ab initio simulations to test the possible role of $e^{2-}_{2,hyd}$ as an intrinsic part of the reaction mechanism. First, Landman and co-workers[16] did a simulation based on density functional theory (DFT) using the PBE exchange−correlation functional[40] and studied what happened when two excess electrons were placed onto an isolated water cluster. These researchers found that the configuration with both electrons separately bound to the cluster surface was slightly more enthalpically favored than the structure where both electrons were colocalized to the same cavity in the cluster interior.[16] By using steered first-principles Born−Oppenheimer molecular dynamics, they also found that the colocalized electrons were able to concertedly extract two protons from two nearby waters to directly produce H_2.

More recently, Bu and co-workers[15] performed DFT-based simulations using the hybrid PBE0 functional[41] with periodic boundary conditions, to represent bulk water, plus two excess electrons. These researchers ran multiple trajectories and found that, although two excess electrons could be separately solvated in two different cavities as two single e^{-}_{hyd}'s, having both electrons localized in a single cavity to form $e^{2-}_{2,hyd}$ was more stable. They also found that only formation of a hydrated dielectron led to the DEHE reaction.[15] That is, solvent-separated electron pairs were not observed to react with water. Interestingly, the mechanism they observed involved sequential proton transfers with a hydride subintermediate

$$e^{-}_{hyd} + e^{-}_{hyd} \rightarrow e^{2-}_{2,hyd} \quad (2)$$

$$e^{2-}_{2,hyd} + H_2O \rightarrow H^- + OH^- \quad (3)$$

$$H^- + H_2O \rightarrow H_2 + OH^- \quad (4)$$

where we refer to reaction 2 as the recombination reaction, reaction 3 as the first proton transfer step (PT-1), and reaction 4 as the second proton transfer step (PT-2).

All of this leads to the series of questions about the mechanism of the DEHE reaction that we explore via DFT-based simulations in this paper. First, are the proton extractions in the DEHE reaction sequential or concerted? Second, instead of simulating water with two excess electrons from the beginning, what happens if a second electron is injected in the presence of an already-equilibrated hydrated electron?[37] This is a scenario that could potentially be explored in pump−probe experiments, and the presence of a well-defined zero of time also allows us to better understand the lifetime of the $e^{2-}_{2,hyd}$ intermediate. Finally, what determines the identities of the first and second protons to be extracted, as well as the lifetime of the potential H^- subintermediate?

Here, we work to answer these questions by running an ensemble of ab initio trajectories using DFT with the PBE0[41] exchange correlation functional in a fully periodic system of 64 water molecules. Rather than vertically injecting two excess charges at the same time, we added a second excess charge to a system with an already equilibrated single e^{-}_{hyd}. We find that the time from injection of the second electron to the time of PT-1 varies from ∼130 fs to nearly ∼1.5 ps. We also see that the duration of reaction (i.e., the time between PT-1 and PT-2 or the H^- lifetime) also showed significant variation between 30 and 130 fs, indicating that the proton transfers can occur either sequentially or effectively concertedly. Next, we see that the first proton to be abstracted must be on a water molecule that not only has significant electron density from $e^{2-}_{2,hyd}$ but also is part of an extended H-bond chain with neighboring waters. This is necessary to allow the newly formed hydroxide ion to be driven away from the H^- subintermediate on time scales faster than standard diffusion. Finally, we find that PT-2 is mediated both by solvation of the hydride subintermediate and by O−H bond lability. Overall, this work presents a deeper understanding of the mechanism of DEHE reaction.

METHODS

To simulate the formation of hydrated dielectrons and the subsequent DEHE reaction via sequential injection of an excess electron into an already equilibrated single-electron system, we used starting configurations from our previously published DFT-based e^{-}_{hyd} simulations.[8,11,23] These simulations were done with the CP2K[42] software package in the *N*, *V*, *T* ensemble at a temperature of 298 K. A time step of 0.5 fs was used, and a Nose−Hoover[43] chain thermostat was coupled to the system to maintain the target temperature. The volume of the system was chosen to reproduce the correct experimental density of water at 298 K and 1 atm. The PBE0[41] exchange−correlation functional was used with 25% exact exchange (note that the related simulations in refs 17,44,45 were performed with 40 or 50% exact exchange) and the Grimme's D3 dispersion correction[46] along with a triple-ζ basis set. Hartree−Fock (HF) exchange calculations were expedited by way of an auxiliary density matrix method.[47]

We selected a series of 16 uncorrelated equilibrated initial configurations and then changed the system charge from −1 to −2 and the total spin multiplicity from 2 to 1, thus introducing a second excess electron with the opposite spin of the already-equilibrated hydrated electron. We made this choice since, as mentioned above, triplet H_2 is not bound,[30] suggesting that reactive dielectron species should initially be present as singlet electron pairs. The choice to study only singlet dielectrons is also justified by previous work from Bu and co-workers,[15] who found that the spin-paired singlet state of the dielectron at this level of theory was more stable than the triplet state. Trajectories were propagated after the second electron was injected either until the DEHE reaction was complete or halted after 2.1 ps if no reaction occurred. Visualizations were done using VMD,[48] and the trajectory animations shown in the Supporting Information were generated using an in-house TCL script.

To determine whether or not H-bond chains between water molecules existed, hydrogen bonds were detected using geometric criteria[49] with a donor−acceptor distance of 3.0 Å and a cutoff angle of >150° using an in-house Mathematica[50] script. Hydrogen bond chains were built by identifying alternating donor/acceptor hydrogen bond motifs, starting with selected water molecules in the first solvation shell of the

https://doi.org/10.1021/acs.jctc.4c00780
J. Chem. Theory Comput. 2024, 20, 7337−7346

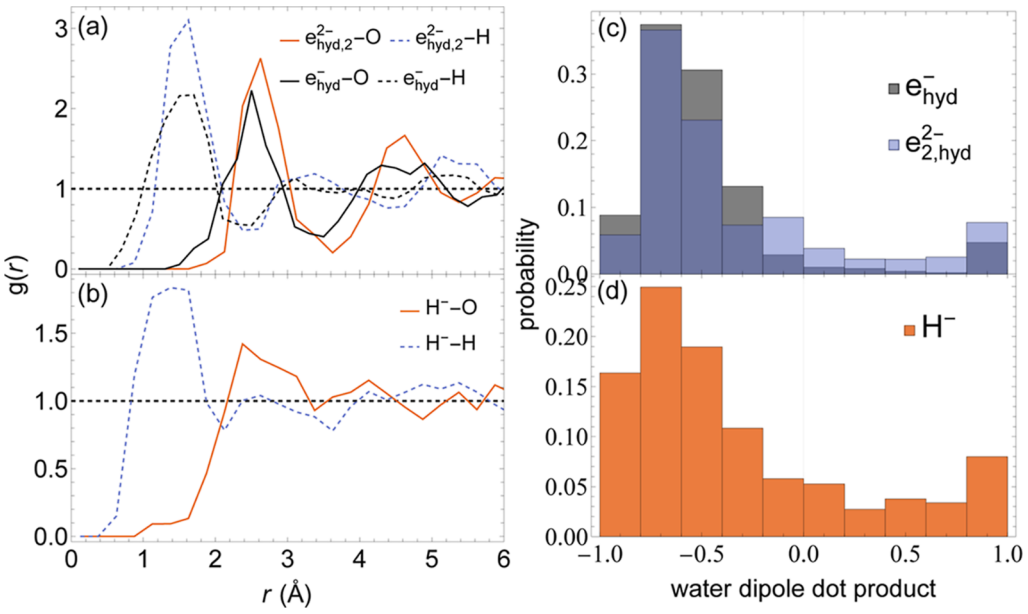

Figure 1. (a) Dielectron (orange and blue curves) and single hydrated electron (black curves) radial distribution functions (RDFs) from the Wannier center to both water oxygen (solid curves) and hydrogen (dashed curves). Dielectron configurations are sampled from before the PT-1 reaction occurs, while the single electron configurations are taken from our previous work.[11] The dielectron shows a slightly larger cavity region than the single electron, but otherwise the two species have similar solvation structures. (b) RDFs of the hydride subintermediate with water O (orange curve) and H (blue dashed curve) during the reaction period between PT-1 and PT-2. Although H^- largely "inherits" the solvation structure of $e^{2-}_{2,hyd}$ because many waters do not have time during the reaction duration to solvate hydride, we do see that H^- is smaller than $e^{2-}_{2,hyd}$ because of electrostatic attraction to the central proton. Moreover, since the H^- proton often resides slightly off-center of the dielectron's cavity, the second- and third-shell peaks are mostly washed out. (c) Angular distributions of first-shell waters for both the single e^-_{hyd} (black bars) and the $e^{2-}_{2,hyd}$ (blue bars). Values near −0.70 indicate solvation by waters with H-bonds pointed toward the (di)electron center. Both structures are highly ordered, with the single electron being slightly more ordered than the dielectron. (d) Angular distributions of first-shell waters for the H^- subintermediate (orange bars). The slightly broader distribution relative to the parent $e^{2-}_{2,hyd}$ is likely due to incomplete equilibration, as H^- only lives for tens to ∼100 fs.

dielectron or hydride. We found, as with previous work in the literature,[51] that hydroxide motion by Grotthus-type proton "hopping" only occurred in the presence of pre-existing extended H-bond chains.

As part of our investigation of the DEHE reaction mechanism, we also explored how the second proton abstraction to form H_2 was displaced from the proton motion to form the H^- subintermediate. We first defined an O−H lengthening vector at the time of PT-1

$$\vec{r}_{OH,PT\text{-}1} = \vec{r}_{H_i,PT\text{-}1} - \vec{r}_{O_i,PT\text{-}1}$$

and then computed hydride displacement vectors over the reaction duration

$$\vec{d}_{H^-,i} = \vec{r}_{H^-,i} - \vec{r}_{H^-,i-1}$$

where $\vec{r}_H$, $\vec{r}_{H^-}$, and $\vec{r}_O$ are hydrogen, hydride, and oxygen positions and i represents a time-step after PT-1 and before PT-2. These vectors were then normalized and their dot product taken at every step of the reaction duration to determine the relative displacement. This hydride displacement measure is shown pictorially and discussed further in conjunction with Figure 5, below; the dot product vs time plots for each individual trajectory are shown in the Supporting Information.

RESULTS AND DISCUSSION

We began our investigation of the DEHE reaction process by first considering the recombination step of the proposed mechanism, eq 2. Following injection of a second, spin antiparallel, excess electron into our simulated system that contained a hydrated electron, we found that in every trajectory, the second electron immediately localized into the same solvent cavity and spatial orbital as the first. We have argued, based on both experiments and simulations, that injected electrons are trap seeking,[52] so it makes sense that the pre-existing hydrated electron's cavity serves as a highly stable trap into which the second electron can colocalize. Thus, if diffusion is not required to bring the two separately solvated electrons into proximity (i.e., if the second electron is injected) and the two electrons have opposite spin, the recombination step happens essentially instantaneously. This suggests a potential experimental route to controllably forming dielectrons, by injecting additional electrons in the presence of already-equilibrated hydrated electrons.[37] This also means that we can controllably form solvated dielectrons in simulations, allowing us to investigate the structure of this important intermediate during the period between recombination and PT-1.

In our previous simulations on single hydrated electrons,[8,23] we were able to track the e^-_{hyd} using either the spin density or the localized singly occupied molecular orbital (SOMO) density. This approach does not work for a dielectron system with two spin antiparallel excess electrons and thus a net zero spin, so here we locate the dielectron utilizing Maximally-Localized Wannier Functions (MLWFs) of the two highest-energy orbitals, calculated directly in CP2K.[42] The orbital centers of the MLWFs are then used as the center of the dielectron. Figure 1a shows radial distribution functions (RDFs or $g(r)$'s) of $e^{2-}_{2,hyd}$ before the PT-1 step of the DEHE reaction takes place, along with the RDFs of the e^-_{hyd} taken from our previous simulations.[8,11] We note that the single hydrated electron RDF shown here differs slightly from the RDF in our past

https://doi.org/10.1021/acs.jctc.4c00780
J. Chem. Theory Comput. 2024, 20, 7337−7346

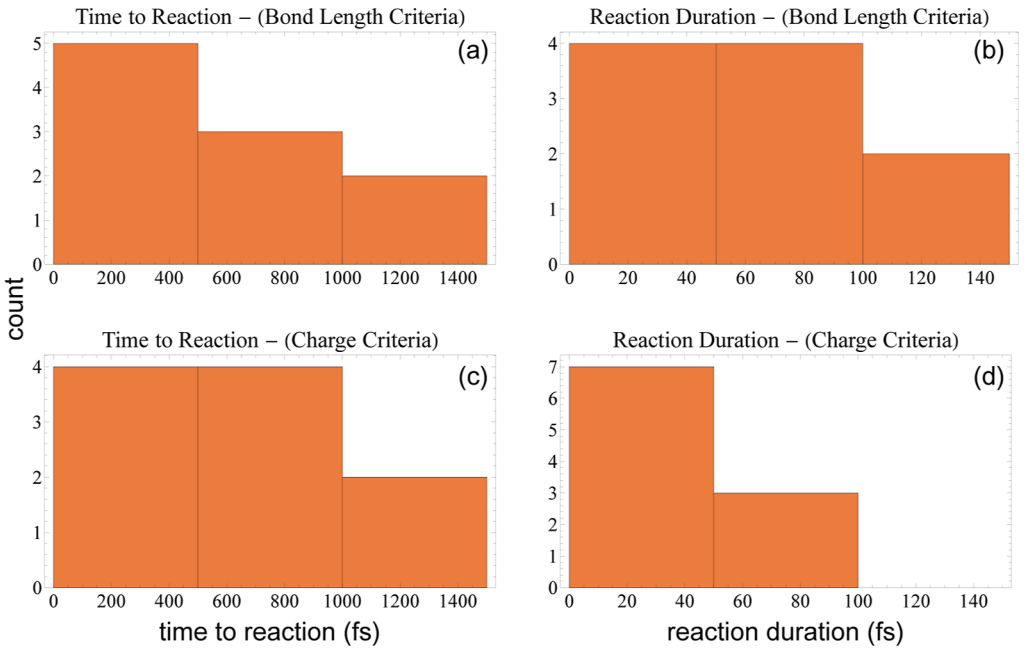

Figure 2. Distributions of times to reaction (panels a and c) and reaction durations (panels b and d) in fs using both the bond length reaction criterion (panels a and c) and the charge reaction criterion (panels b and d). The time to reaction is the time from injection of the second hydrated electron to the onset of PT-1, and the reaction duration is the time between PT-1 and PT-2. Use of the bond length reaction criterion shifts the reaction duration to longer time scales, indicating that fluctuations in charge occurring between PT-1 and PT-2 precede significant bond length changes for the second reactive water. This indicates that electron density donation into the water antibonding orbitals increased the lability of O−H bonds, thus making them more primed for reaction.

work[8,23] because here we also use MLWFs to track the electron center for better comparison, rather than the SOMO used in our previous work.

Figure 1a makes clear that the central cavity region of the dielectron is slightly larger than that of the single hydrated electron, as seen by the distance where the $e^{2-}_{2,hyd}$−water oxygen $g(r)$ first becomes nonzero. We obtain a radius of gyration (R_g) for the dielectron of 2.91 ± 0.17 Å, which is in qualitative agreement with the value cited by Bu and co-workers,[15] and is 24% larger than that of the single hydrated electron (R_g = 2.35 ± 0.09 Å) simulated at this level of theory. As above, we note that this single electron radius of gyration differs slightly from what we have previously published[8,11,23] because it was calculated using the MLWF density as opposed to the SOMO. The first solvation shell peak, however, is nearly identical for both the single and di-hydrated electron species, suggesting that addition of a second electron causes only minor changes in the local solvent structure beyond a slight expansion of the central cavity.

The histograms in Figure 1c show the angular distributions of the first-shell water molecules around both the single hydrated electron and the dielectron, calculated as the dot product of the unit vector connecting the dielectron center of mass to the water O atom with a unit vector along the water dipole. With this definition, a dot product of ∼−0.7 is characteristic of water pointing an O−H bond toward the (di)electron center of mass. Thus, the sharp peak seen near −0.70 in both the single e^{-}_{hyd} and the dielectron distribution is indicative of a very highly structured solvation shell. Interestingly, the dielectron seems slightly less structured than the single electron, which would not be expected given the increased charge of the $e^{2-}_{2,hyd}$ relative to that of a single e^{-}_{hyd}. It is possible that this simply reflects incomplete equilibration of the dielectron, as the subsequent reactivity with water limits the equilibration time of the first solvation shell. Despite this, the data in Figure 1 indicate that up until the onset of PT-1, hydrated electrons and dielectrons are similarly solvated by the surrounding water.

Of the 16 nonequilibrium trajectories that we ran, 10 of them underwent the DEHE reaction within 2.1 ps of injection of the second electron. Since there is no single definition that determines precisely when a chemical reaction takes place, we utilized both a "bond length criterion" and a "charge criterion" to estimate precisely when each step of the reaction occurred. For the bond length criterion, we defined the start of the reaction (and thus the time of PT-1) as the moment where the first reacting water's O−H bond length begins to monotonically increase from its equilibrium value. We then deemed that the DEHE reaction is finished when the bond length of the newly formed H_2 reaches its equilibrium value. For the charge criterion, we defined PT-1 as the moment when the net charge on the O atom of the first reacting water passes a threshold consistent with it being identified as a hydroxide ion (see the Supporting Information for details on charge analyses). We then defined the end of the DEHE reaction as when the net charge on the O atom of the second reacting water achieves this same threshold value. We see that stretching of the O−H bond of the reactive waters occurs several time steps before the charge finishes flowing onto either molecular fragment.

The distinction of these two reaction criteria is important as they allow us to track different stages of the reaction mechanism around the time of PT-1. When using the bond length criterion, hydride has not yet completely formed and the $e^{2-}_{2,hyd}$ still exists, therefore we can study how the dielectron donates charge density onto the first reacting water and the impact this has on O−H bond breaking. This is a because O−H bond lengthening precedes the charge flow that starts to reduce water to OH^-. The charge criterion, on the other hand, directly indicates when hydride has formed (i.e., that the $e^{2-}_{2,hyd}$ has just reacted to form

https://doi.org/10.1021/acs.jctc.4c00780
J. Chem. Theory Comput. 2024, 20, 7337−7346

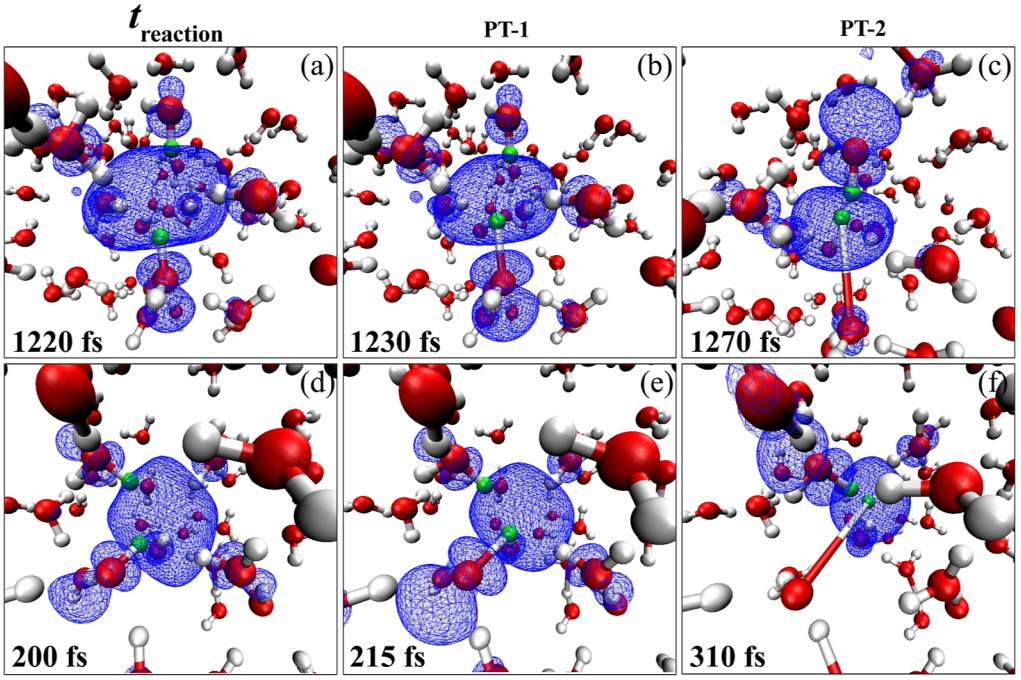

Figure 3. Snapshots of two representative DEHE reaction trajectories as a function of time from injection of the second electron. The system is shown just before PT-1 takes place (panels a and d), as PT-1 takes place (panels b and e) and as PT-2 takes place (panels c and f). Oxygen atoms of water molecules are shown in red, while H atoms are shown in gray. Reactive H atoms are highlighted in green, and the square of the Wannier function for the two highest occupied orbitals are shown as the blue isosurface mesh. This density corresponds to the $e^{2-}_{2,hyd}$ before PT-1 takes place, and then represents the H^- ion during the time between PT-1 and PT-2. Before PT-1 takes place, the reacting waters are across the dielectron cavity from each other in the trajectory shown in a, while they are adjacent to each other in the trajectory shown in d. In both trajectories, significant donation of dielectron density onto the first reacting water precedes reaction, and during PT-1 a proton from the first reacting water falls into the $e^{2-}_{2,hyd}$ center, forming H^-. PT-2 is preceded by donation of H^- electron density onto the second reacting water molecule. The reaction duration (time between PT-1 and PT-2) varies significantly for these two trajectories, due to details of the hydride solvation (see text for discussion).

H^- and OH^-), allowing us a way to study the solvation and other dynamics of the hydride ion.

Figure 2 shows distributions of both the time to the start of the DEHE reaction (i.e., the time from injection of the second electron to PT-1, left panels) as well as the reaction duration (i.e., the H^- lifetime, which is the time from PT-1 to the end of the DEHE reaction, right panels), defined with both the bond length (upper panels) and charge (lower panels) criteria. Although the distributions do depend somewhat on the chosen criterion, the data show clearly that the DEHE reaction occurs on time scales of hundreds of fs up to a few ps. The duration of the reaction also varies significantly, ranging from just a few fs to over 100 fs. Thus, the disagreement between Bu and co-workers[15] and Landman and co-workers[16] on whether the two DEHE reaction proton transfers occur sequentially or concurrently is likely due to insufficient sampling of reaction dynamics, particularly with only a single trajectory being explored in ref 16. We will argue below that the distribution of reaction times occurs because of solvation effects that can either promote concurrent proton transfers or delay the second transfer long enough for H^- to live as a transient subintermediate.

Figure 3 shows representative snapshots of two DEHE reactive trajectories at the time just before reaction (panels a and d), during PT-1 (panels b and e), and during PT-2 (panels c and f); here, the reactive protons are shown in green and the dielectron MLWF charge density is shown as a blue mesh isosurface. Movies of two representative reactive trajectories are available in the Supporting Information. The trajectory shown in panels (a–c) bears a strong resemblance to the one presented by Landman and co-workers,[16] in that the two reacting waters are roughly opposite each other across the dielectron cavity and there is little time between the two proton transfers. In the trajectory shown in panels (d–f), however, the two protons are not transferred concertedly, and the reacting waters are adjacent, indicating that a cross-cavity geometry is not necessary for the DEHE reaction to occur. Analysis of our reactive ensemble shows that 4 out of 10 trajectories have an angle between the two reactive waters (relative to the dielectron center of mass) between 100 and 120°, with 5 trajectories having angles larger than 120° and one having an angle of only 90°. We also found no correlation between the reaction duration (i.e., how concerted the two proton transfers are) and the positions of the reacting waters, suggesting that the time between the two proton transfers is controlled by something other than simple geometry.

The snapshots in Figure 3 and the movies in the SI show that after PT-1, the first reacting proton essentially falls into the center of the dielectron density to form the H^- subintermediate. This hydride ion is what then goes on to initiate PT-2, leading to the formation of molecular hydrogen and completion of the DEHE reaction. As seen in Figure 3b, there is significantly more electron density donated onto the first reacting water than all the other waters in the first shell, and we see this type of density donation for every PT-1 event in our ensemble. This density ends up as part of the H^- ion before shifting to reside on the second reacting water. This indicates that donation of excess $e^{2-}_{2,hyd}$ electron density into water antibonding orbitals is part of what makes the O–H bond of the reacting water more labile, a process that cannot occur when only a single electron is present

https://doi.org/10.1021/acs.jctc.4c00780
J. Chem. Theory Comput. 2024, 20, 7337–7346

in the cavity, which limits the amount of potential charge donation.

Analysis of our DEHE trajectories shows that although electron density donation onto reacting waters is necessary for both proton transfer steps to occur, it is not sufficient: for PT-1 in particular, there are many instances where a significant part of the dielectron density resides on a neighboring water but proton transfer does not occur. To understand why this is the case, we investigated the role of hydrogen bonding in promoting reactivity for both proton transfer steps. Figure 4 shows the

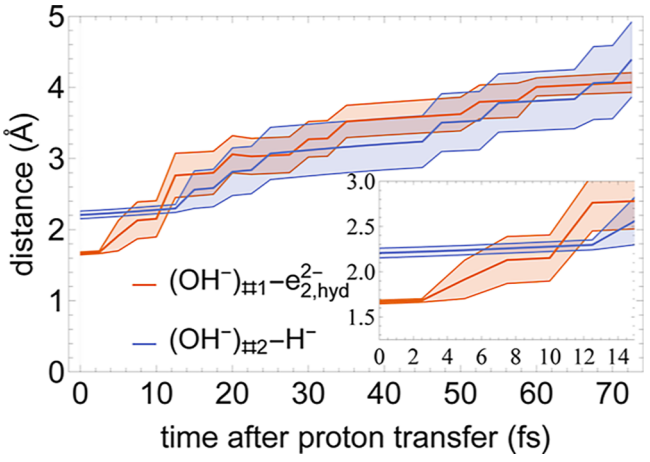

Figure 4. $(OH^-)_{\#1}$ and $(OH^-)_{\#2}$ distances from the reaction center as a function of time after proton transfer. The reaction center for $(OH^-)_{\#1}$ is defined as the Wannier center of mass of $e^{2-}_{2,hyd}$, while the reaction center for $(OH^-)_{\#2}$ is the proton at the center of the hydride ion. Error bars are calculated as the standard error of the mean. $(OH^-)_{\#1}$ shows rapid, driven motion away from the reaction center, mediated by hydroxide hops down extended H-bond chains. $(OH^-)_{\#2}$, on the other hand, shows more diffusive movement.

ensemble-averaged displacement of the hydroxide ions created immediately following PT-1 and PT-2; for PT-1, the origin was taken as the $e^{2-}_{2,hyd}$ center of mass, while for PT-2 the origin was the proton of the H^- subintermediate. The hydroxide produced from PT-1, denoted $(OH^-)_{\#1}$, shows driven motion away from the reaction center. This motion takes place through rapid proton transfers (i.e., a Grotthuss-like mechanism)[53] via proton hopping along an H-bond chain. Conversely, the hydroxide created from PT-2, denoted $(OH^-)_{\#2}$, moves at the rate expected for hydroxide diffusion (i.e., with both physical and proton hopping motions) with this level of theory.[51] In other words, the proton-transfer-induced hopping rate for $(OH^-)_{\#1}$ immediately upon creation is roughly five times that observed for $(OH^-)_{\#2}$.

This observation suggests that the PT-1 step cannot take place unless there is a pre-existing H-bond chain that can help the charge associated with $(OH^-)_{\#1}$ get at least one solvent shell away from the reaction center in the first ∼20 fs. This makes sense given that the water donating the first proton lies in the dielectron's first solvent shell, so that $(OH^-)_{\#1}$ forms directly in the first shell of the newly created H^- subintermediate, leading to a strong electrostatic repulsion between the two adjacent negatively charged species. Since this repulsion is unfavorable, PT-1 does not occur until there is not only enough charge density on the first-shell water but also that the first-shell water is part of an H-bond chain that allows the hydroxide to quickly move at least one solvent shell away by proton hopping. This dual requirement explains the large dispersion in times for the onset of PT-1 following formation of the $e^{2-}_{2,hyd}$. Landman and co-workers[16] also noted hopping of the resulting hydroxides after the proton transfer step, but they did not comment on any accelerated motion or how OH^- hopping could impact reactivity.

To confirm that the presence of an H-bond chain is required for the PT-1 reaction to occur, we used a geometric criterion[49] to detect the presence of H-bonds between water molecules; see the Methods section and Supporting Information for details. We then defined hydrogen bond chains as collections of H-bonds that begin at a given first-shell water and alternate through H-bond donor and acceptor motifs. We found that at the time of PT-1, the reacting water always had a hydrogen bond chain with a length of at least 4 waters, with some reacting waters having chain lengths up to 10 waters. We also saw instances when there was significant electron donation onto a first shell water but no reaction occurred because no H-bond chain was connected to that water at that time; examples of this are detailed in Figure S6 of the Supporting Information. This verifies that PT-1 is mediated by H-bond chain formation, which is required both to better stabilize $(OH^-)_{\#1}$ immediately upon its formation as well as to mitigate the electrostatic repulsion with H^- by providing a proton hopping pathway to superdiffusively move this hydroxide farther away.

For PT-2, on the other hand, $(OH^-)_{\#2}$ is formed adjacent to a neutral H_2 molecule, and given that $(OH^-)_{\#1}$ has already been driven far from the reaction center, there is no electrostatic need for an H-bond chain to drive rapid hydroxide displacement, and indeed, none is observed. This is consistent with our H-bond analysis, which showed that the PT-2 reacting water did not always have a ≥ 4-water H-bond chain at the time of reaction, discussed in more detail in the Supporting Information. Since needing an H-bond chain is not required, this leads to the question of what causes the dispersion in the reaction duration times seen in Figure 2b,d.

We believe that the H^- lifetime is also determined by geometric criteria. After PT-1, the proton falls to the center of the $e^{2-}_{2,hyd}$, so the newly created hydride effectively "inherits" the dielectron's solvation structure; indeed, Figure S1 in the Supporting Information shows that $e^{2-}_{2,hyd}$ and H^- have similar first-shell water coordination numbers. Figure 1b shows RDFs of the hydride ion subintermediate, although we note that this solvation structure is not equilibrated given the short average lifetime of H^-. This figure shows that the first solvent shell peak of H^- closely matches that of $e^{2-}_{2,hyd}$, verifying that the hydride solvation structure is very similar to that of the dielectron. This is further supported by the water dipole distribution in Figure 1d, which shows that H^-, which is only singly negatively charged, orders the surrounding waters only slightly less that the doubly negatively charged dielectron. Since the hydride subintermediate is a singly charged anion with a proton at the center, the spatial extent of the charge density of H^- is smaller than the $e^{2-}_{2,hyd}$; this means that hydride puts less charge density onto the first-shell water molecules. This suggests that PT-2 cannot take place until a first-shell water can move inward enough to have enough charge density for the reaction to take place, placing at least one restriction on when the DEHE reaction can go to completion.

We also found that, in addition to having waters at an appropriate distance from H^- to react, the relatively wide distribution of reaction durations also results from other aspects of hydride solvation following PT-1. To see this, we investigated

https://doi.org/10.1021/acs.jctc.4c00780
J. Chem. Theory Comput. 2024, 20, 7337−7346

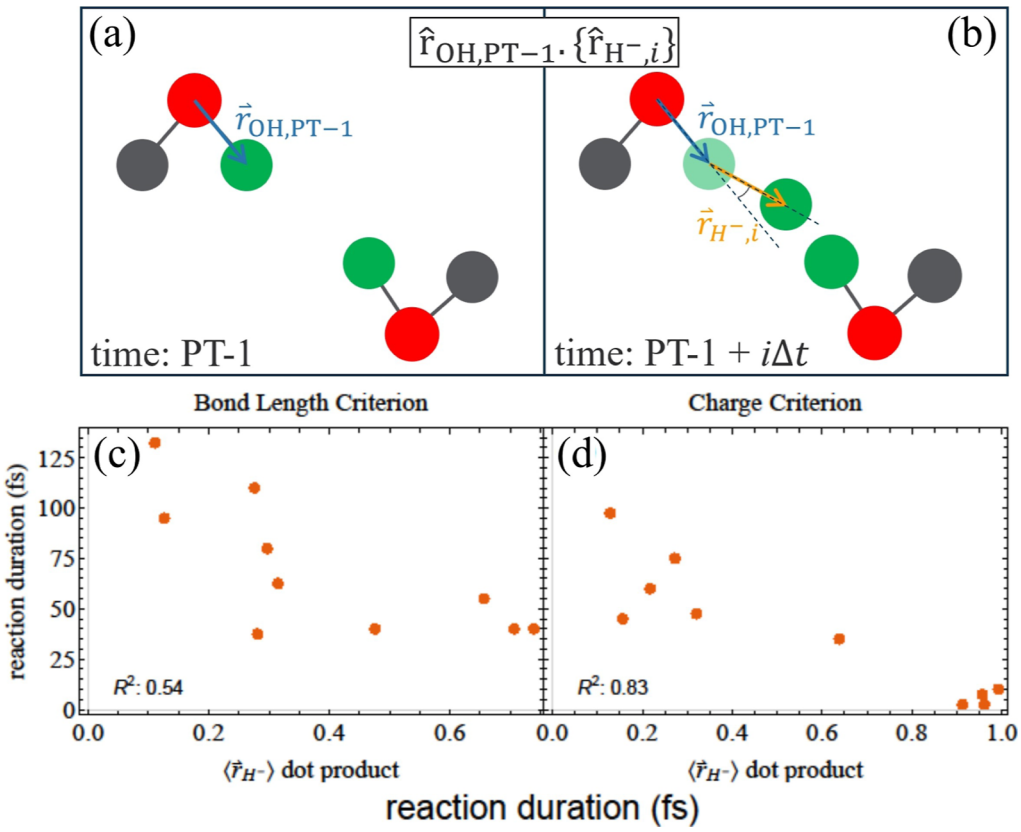

Figure 5. Correlation between hydride displacement and the reaction duration (time between PT-1 and PT-2). At the time of PT-1 (panel a, with O atoms shown in red, H atoms in gray and the reactive protons in green), we define the O−H lengthening vector as a unit vector along the O−H bond of the water that loses the first proton. We then define (panel b) an H^- displacement vector as a unit vector along the difference in the positions of the hydride proton at time step i (green proton on upper water) and the previous time step (translucent green proton on upper water). We then determine the displacement as the dot product between these two unit vectors at each time step. Scatter plots of the average hydride displacement measure vs reaction duration are shown for the bond length (panel c) and charge criteria (panel d). Both criteria show a significant negative correlation, with a particularly strong correlation for the charge criterion. This is because hydride does not fully exist at the start of the reaction duration for the bond length criterion. This means that time steps where the reactive proton has not yet become H^- are contributing to the displacement in a spurious way.

the translational displacement of the abstracted proton following PT-1 as it first becomes hydride and then reacts via PT-2 to form H_2 (see the Methods section and Figure 5a,b for an illustration of this analysis). In some trajectories, the first reactive proton becomes H^- by following a path straight along its original O−H bond vector until it reacts with a proton from a second water molecule to form H_2. In other trajectories, however, the first proton deviates from its initial O−H bond lengthening path. This deviation could result physically, by deflection of the first proton by other nearby water molecules, or could result from the absence of a sufficiently reactive partner, either due to there being no protons along its trajectory or due to those protons having insufficient O−H bond lability. When such deviations occur, the surrounding waters then solvate the newly formed H^- until a reactive partner is found and H_2 can form.

To verify that deviations like this are involved in the distribution of reaction durations, we calculated the distribution of deviations of the abstracted proton from its original O−H lengthening vector (defined at PT-1) over the time period between PT-1 and PT-2; the way we calculate the deviation is defined in the Methods section and shown pictorally in Figure 5 panels (a,b), with further details given in the Supporting Information. Values of the deviation close to 1 indicate that the abstracted proton closely follows its original O−H lengthening vector up until PT-2, while smaller values indicate more significant deviation from the original path. As shown in Figure 5 panels (c,d), this measure of proton deviation is inversely correlated with the reaction duration, with a correlation coefficient $R^2 = 0.83$ ($R^2 = 0.54$) for the charge (bond length) reaction duration criterion; time traces of the deviation for individual trajectories are shown in the Supporting Information. Trajectories where the proton that forms hydride is highly deflected go through a more extended period of hydride solvation (tens to hundreds of fs), so that librational motions of neighboring waters are required to eventually promote the onset of PT-2.

Overall, our simulations and analysis provide a new molecular-level understanding of the DEHE reaction process. First, the reaction begins via the coalescence or recombination of two separately solvated hydrated electrons into a single cavity. This process could happen diffusively,[15] or it could be induced by injecting a spin-antiparallel electron into the proximity of a pre-existing hydrated electron.[37] The resulting $e^{2-}_{2,hyd}$ starts to become solvated for a variable amount of time until the PT-1 step occurs. PT-1 is initiated both by the presence of significant donation of electron density from the dielectron onto a nearby water molecule, which enhances O−H bond lability, and by that water being part of an H-bond chain, so that the newly created OH^- product is able to rapidly move away from its H^- partner. There is then a fairly wide distribution of times between the onset of PT-1 and PT-2, which results both from the degree of solvation of the H^- product and the degree to which the initially

https://doi.org/10.1021/acs.jctc.4c00780
J. Chem. Theory Comput. 2024, 20, 7337−7346

abstracted proton is deflected off of its initial O−H bond lengthening path.

CONCLUSIONS

In this work, we presented a detailed investigation of the DEHE reaction using DFT-based ab initio simulations, with the reaction initiated by injecting a second electron in the presence of an existing hydrated electron to impose a well-defined reaction start time. Our results show immediate recombination of spin antiparallel electrons into a single cavity to form a hydrated dielectron; we saw no trajectories where the second electron localized independently of the first. We also found that the reaction proceeds via a multistep process via a hydride subintermediate, but with a range of H^- lifetimes that allowed us to explain the discrepancy between previous DFT-based simulations from other groups.[15,16] We found that the distribution of times from injection of the second electron to the onset of the PT-1 reaction that forms H^- results first from the need for solvation to allow part of the charge density to reside on a single first-shell water, and second from that water being part of an extended H-bond chain so that the newly formed hydroxide ion can move rapidly away from the reaction center to minimize electrostatic repulsion between the OH^- and hydride. The distribution of reaction durations resulted both from the dynamics of solvation of the newly created hydride and the relative degree of mis-alignment of the abstracted proton with its initial trajectory following elongation of an O−H bond.

We believe that the observations above can help to rationalize the significant isotope effect[29,31,54−56] seen for this reaction, which strongly favors formation of H_2 over D_2 in H_2O/D_2O mixtures, as well as the unusual temperature dependence of the reaction rate.[3] Of course, the zero point energy difference between O−H and O−D bonds[57,58] contributes to the selective abstraction of protons over deuterons, and the observed isotope effect may simply be a consequence of this difference. However, we also know that D-bonds are stronger than H-bonds, so that motion along and perpendicular to the water−water D-bond distance is reduced in heavy water,[57,58] and these librations are needed to drive H/D-bond chain formation.[59] This means that waters in the first shell of the dielectron may be more likely to rapidly build extended H-bond chains than D-bond chains due to their greater fluctuations, so the fact that our simulations show that H-bond chains are required to separate the like-charged products of the PT-1 reaction also could help explain why this reaction so heavily selects for proton rather than deuteron abstraction. Moreover, it is also possible that zero-point energy differences in O−H and O−D bond strengths could cause an isotope effect for PT-2, where the hydride intermediate more easily abstracts protons over deuterons.

The fact that an H-bond chain is required for the PT-1 step of the reaction to occur also may help explain the reduced rate of the DEHE reaction above 150 °C.[3] One would expect that formation of extended H-bond chains becomes less probable at higher temperatures, possibly explaining why the reaction appears to shut when the temperature is increased. Although the need of H-bond chains may help rationalize the temperature dependence, it is unfortunately not possible for us to comment on the facts that the reaction rate is diffusion limited and independent of ionic strength. This is because our simulations start with the two electrons in the same cavity, so that the nature of how two single electrons recombine and how recombination might be affected by ion pairing with salt are not accessible from our work. Simulations where dielectrons are prepared via diffusive recombination of single electrons, particularly with electron−electron distances greater than the experimentally proposed reaction distance,[30] would be needed to understand these aspects of the reaction, but the system sizes required and the time-scales necessary to observe the DEHE reaction are presently not computationally feasible. Despite this, the work presented here does add to a growing base of literature studying the mechanism of hydrated electron reactivity, including not only the DEHE but also the reduction of a variety of small molecules in solution.[14−16,25,27,28]

We conclude by noting that our previous work studying single hydrated electrons with DFT and the PBE0 functional[11,23] indicated that the solvation structure is too kosmotropic compared to experiment. Since we and others[15,16] have shown that the reacting water molecules are tightly bound in the first shell of the dielectron, this suggests that the simulated dielectron hydration shell also is overstructured, which may artificially shorten both the time to reaction and the reaction duration relative to experiment and/or other levels of theory. We also see that donation of electron density onto first shell waters plays a large role in enhancing O−H bond lability. This means that the mechanisms and time scales that we observe for this simulated reaction will likely depend significantly on the choice of the exchange−correlation functional. Even something as simple as changing the percentage of exact Hartree−Fock exchange in hybrid functionals is known to change the band gap of liquid water,[60,61] which means it would also impact the amount of (di)electron density that can be shared into the first-shell water antibonding orbitals and thus the propensity for proton abstraction. Further studies of dielectron reactivity using other functionals and potentially other levels of theory are needed to fully corroborate ab initio simulations with experimental observations.

ASSOCIATED CONTENT

Supporting Information

The Supporting Information is available free of charge at https://pubs.acs.org/doi/10.1021/acs.jctc.4c00780.

Analysis of dielectron and hydride structure, Hydrogen bond and hydrogen bond chain analyses, Hydroxide hopping and electrostatic repulsion analysis, O−H bond length activation analysis, Wannier density integration analysis, hydride displacement dot product analysis, Reactive water geometry analysis, Reaction animations (PDF)

(MP4)

(MP4)

AUTHOR INFORMATION

Corresponding Author

Benjamin J. Schwartz − *Department of Chemistry & Biochemistry, University of California, Los Angeles Los Angeles, California 90095-1569, United States;* orcid.org/0000-0003-3257-9152; Phone: (310) 206-4113; Email: schwartz@chem.ucla.edu

Authors

William R. Borrelli − *Department of Chemistry & Biochemistry, University of California, Los Angeles Los Angeles, California 90095-1569, United States*

https://doi.org/10.1021/acs.jctc.4c00780
J. Chem. Theory Comput. 2024, 20, 7337−7346

José L. Guardado Sandoval − *Department of Chemistry & Biochemistry, University of California, Los Angeles Los Angeles, California 90095-1569, United States*
Kenneth J. Mei − *Department of Chemistry & Biochemistry, University of California, Los Angeles Los Angeles, California 90095-1569, United States*

Complete contact information is available at: https://pubs.acs.org/10.1021/acs.jctc.4c00780

Notes

The authors declare no competing financial interest.

■ ACKNOWLEDGMENTS

This work was funded by the National Science Foundation under grants CHE-1856050 and CHE-2247583. We thank XSEDE for the necessary computational resources for all calculations involved in this project.

■ REFERENCES

(1) Gordon, S.; Hart, E. J.; Matheson, M. S.; Rabani, J.; Thomas, J. K. Reactions of the hydrated electron. *Discuss. Faraday Soc.* **1963**, *36*, 193−205.
(2) Hart, E. J. The Hydrated Electron. *Science* **1964**, *146*, 19−25.
(3) Marin, T. W.; Takahashi, K.; Jonah, C. D.; Chemerisov, S. D.; Bartels, D. M. Recombination of the Hydrated Electron at High Temperature and Pressure in Hydrogenated Alkaline Water. *J. Phys. Chem. A* **2007**, *111*, 11540−11551.
(4) Herbert, J. M.; Coons, M. P. The Hydrated Electron. *Annu. Rev. Phys. Chem.* **2017**, *68*, 447−472.
(5) Kumar, A.; Becker, D.; Adhikary, A.; Sevilla, M. D. Reaction of Electrons with DNA: Radiation Damage to Radiosensitization. *Int. J. Mol. Sci.* **2019**, *20*, 3998.
(6) Jordan, C. J. C.; Coons, M. P.; Herbert, J. M.; Verlet, J. R. R. Spectroscopy and dynamics of the hydrated electron at the water/air interface. *Nat. Commun.* **2024**, *15*, 182.
(7) Park, S. J.; Schwartz, B. J. How Ions Break Local Symmetry: Simulations of Polarized Transient Hole Burning for Different Models of the Hydrated Electron in Contact Pairs with Na+. *J. Phys. Chem. Lett.* **2023**, *14*, 3014−3022.
(8) Borrelli, W. R.; Mei, K. J.; Park, S. J.; Schwartz, B. J. Partial Molar Solvation Volume of the Hydrated Electron Simulated Via DFT. *J. Phys. Chem. B* **2024**, *128*, 2425−2431.
(9) Narvaez, W. A.; Park, S. J.; Schwartz, B. J. Competitive Ion Pairing and the Role of Anions in the Behavior of Hydrated Electrons in Electrolytes. *J. Phys. Chem. B* **2022**, *126*, 7701−7708.
(10) Casey, J. R.; Schwartz, B. J.; Glover, W. J. Free Energies of Cavity and Noncavity Hydrated Electrons Near the Instantaneous Air/Water Interface. *J. Phys. Chem. Lett.* **2016**, *7*, 3192−3198.
(11) Park, S. J.; Schwartz, B. J. Understanding the Temperature Dependence and Finite Size Effects in Ab Initio MD Simulations of the Hydrated Electron. *J. Chem. Theory Comput.* **2022**, *18*, 4973−4982.
(12) Park, S. J.; Schwartz, B. J. Evaluating Simple Ab Initio Models of the Hydrated Electron: The Role of Dynamical Fluctuations. *J. Phys. Chem. B* **2020**, *124*, 9592−9603.
(13) Ahmadi, S. Hydrated electrons and cluster science. *J. Mol. Struct.* **2022**, *1250*, 131898.
(14) Neupane, P.; Bartels, D. M.; Thompson, W. H. Exploring the Unusual Reactivity of the Hydrated Electron with CO2. *J. Phys. Chem. B* **2024**, *128*, 567−575.
(15) Gao, L.; Zhang, L.; Fu, Q.; Bu, Y. Molecular Dynamics Characterization of Dielectron Hydration in Liquid Water with Unique Double Proton Transfers. *J. Chem. Theory Comput.* **2021**, *17*, 666−677.
(16) Barnett, R. N.; Giniger, R.; Cheshnovsky, O.; Landman, U. Dielectron Attachment and Hydrogen Evolution Reaction in Water Clusters. *J. Phys. Chem. A* **2011**, *115*, 7378−7391.
(17) Pizzochero, M.; Ambrosio, F.; Pasquarello, A. Picture of the wet electron: a localized transient state in liquid water. *Chem. Sci.* **2019**, *10*, 7442−7448.
(18) Lan, J.; Rybkin, V. V.; Pasquarello, A. Temperature Dependent Properties of the Aqueous Electron. *Angew. Chem., Int. Ed.* **2022**, *61*, No. e202209398.
(19) Anbar, M.; Alfassi, Z. B.; Bregman-Reisler, H. Hydrated Electron Reactions in View of Their Temperature Dependence. *J. Am. Chem. Soc.* **1967**, *89*, 1263−1264.
(20) Novelli, F.; Chen, K.; Buchmann, A.; Ockelmann, T.; Hoberg, C.; Head-Gordon, T.; Havenith, M. The birth and evolution of solvated electrons in the water. *Proc. Natl. Acad. Sci. U.S.A.* **2023**, *120*, No. e2216480120.
(21) Bragg, A. E.; Verlet, J. R. R.; Kammrath, A.; Cheshnovsky, O.; Neumark, D. M. Hydrated Electron Dynamics: From Clusters to Bulk. *Science* **2004**, *306*, 669−671.
(22) Svoboda, V.; Michiels, R.; LaForge, A. C.; Med, J.; Stienkemeier, F.; Slavíček, P.; Wörner, H. J. Real-time observation of water radiolysis and hydrated electron formation induced by extreme-ultraviolet pulses. *Sci. Adv.* **2020**, *6*, No. eaaz0385.
(23) Park, S. J.; Narvaez, W. A.; Schwartz, B. J. Ab Initio Studies of Hydrated Electron/Cation Contact Pairs: Hydrated Electrons Simulated with Density Functional Theory Are Too Kosmotropic. *J. Phys. Chem. Lett.* **2023**, *14*, 559−566.
(24) Uhlig, F.; Marsalek, O.; Jungwirth, P. Unraveling the Complex Nature of the Hydrated Electron. *J. Phys. Chem. Lett.* **2012**, *3*, 3071−3075.
(25) Marsalek, O.; Uhlig, F.; VandeVondele, J.; Jungwirth, P. Structure, Dynamics, and Reactivity of Hydrated Electrons by Ab Initio Molecular Dynamics. *Acc. Chem. Res.* **2012**, *45*, 23−32.
(26) Fennell, B. D.; Fowler, D.; Mezyk, S. P.; McKay, G. Reactivity of Dissolved Organic Matter with the Hydrated Electron: Implications for Treatment of Chemical Contaminants in Water with Advanced Reduction Processes. *Environ. Sci. Technol.* **2023**, *57*, 7634−7643.
(27) Rybkin, V. V. Mechanism of Aqueous Carbon Dioxide Reduction by the Solvated Electron. *J. Phys. Chem. B* **2020**, *124*, 10435−10441.
(28) Huyen, T. L.; Pham, T. V.; Nguyen, M. T.; Lin, M. C. A model study on the mechanism and kinetics for reactions of the hydrated electron with H3O+ and NH4+ ions. *Chem. Phys. Lett.* **2019**, *731*, 136604.
(29) Han, P.; Bartels, D. M. Hydrogen/deuterium isotope effects in water radiolysis. 4. The mechanism of aquated hydrogen atom.dblharw. solvated electron [(H)aq.dblharw. (e-)aq] interconversion. *J. Phys. Chem.* **1992**, *96*, 4899−4906.
(30) Schmidt, K. H.; Bartels, D. M. Lack of ionic strength effect in the recombination of hydrated electrons (e)aq + (e)aq → 2(OH) + H2. *Chem. Phys.* **1995**, *190*, 145−152.
(31) Hart, E.; Anbar, M. *The Hydrated Electron*; Wiley-Interscience, 1970.
(32) Basco, N.; Kenney-Wallace, G. A.; Vidyarthi, S. K.; Walker, D. C. A Transient Intermediate in the Bimolecular Reaction of Hydrated Electrons. *Can. J. Chem.* **1972**, *50*, 2059−2070.
(33) Basco, N.; Kenney, G. A.; Walker, D. C. Formation and photodissociation of hydrated electron dimers. *J. Chem. Soc. D* **1969**, 917−918.
(34) Larsen, R. E.; Schwartz, B. J. Full Configuration Interaction Computer Simulation Study of the Thermodynamic and Kinetic Stability of Hydrated Dielectrons. *J. Phys. Chem. B* **2006**, *110*, 1006−1014.
(35) Larsen, R. E.; Schwartz, B. J. Mixed Quantum/Classical Molecular Dynamics Simulations of the Hydrated Dielectron: The Role of Exchange in Condensed-Phase Structure, Dynamics, and Spectroscopy. *J. Phys. Chem. B* **2004**, *108*, 11760−11773.
(36) Larsen, R. E.; Schwartz, B. J. Nonadiabatic Molecular Dynamics Simulations of Correlated Electrons in Solution. 1. Full Configuration Interaction (CI) Excited-State Relaxation Dynamics of Hydrated Dielectrons. *J. Phys. Chem. B* **2006**, *110*, 9681−9691.
(37) Larsen, R. E.; Schwartz, B. J. Nonadiabatic Molecular Dynamics Simulations of Correlated Electrons in Solution. 2. A Prediction for the

Observation of Hydrated Dielectrons with Pump-Probe Spectroscopy. *J. Phys. Chem. B* **2006**, *110*, 9692−9697.
(38) Kaukonen, H.; Barnett, R. N.; Landman, U. Dielectrons in water clusters. *J. Chem. Phys.* **1992**, *97*, 1365−1377.
(39) Hartweg, S.; Barnes, J.; Yoder, B. L.; Garcia, G. A.; Nahon, L.; Miliordos, E.; Signorell, R. Solvated dielectrons from optical excitation: An effective source of low-energy electrons. *Science* **2023**, *380*, 1161−1165.
(40) Perdew, J. P.; Burke, K.; Ernzerhof, M. Generalized Gradient Approximation Made Simple. *Phys. Rev. Lett.* **1996**, *77*, 3865−3868.
(41) Perdew, J. P.; Ernzerhof, M.; Burke, K. Rationale for mixing exact exchange with density functional approximations. *J. Chem. Phys.* **1996**, *105*, 9982−9985.
(42) Kühne, T. D.; Iannuzzi, M.; Del Ben, M.; Rybkin, V. V.; Seewald, P.; Stein, F.; Laino, T.; Khaliullin, R. Z.; Schütt, O.; Schiffmann, F.; et al. CP2K: An electronic structure and molecular dynamics software package - Quickstep: Efficient and accurate electronic structure calculations. *J. Chem. Phys.* **2020**, *152*, 194103.
(43) Martyna, G. J.; Klein, M. L.; Tuckerman, M. Nosé−Hoover chains: The canonical ensemble via continuous dynamics. *J. Chem. Phys.* **1992**, *97*, 2635−2643.
(44) Ambrosio, F.; Miceli, G.; Pasquarello, A. Electronic Levels of Excess Electrons in Liquid Water. *J. Phys. Chem. Lett.* **2017**, *8*, 2055−2059.
(45) Wilhelm, J.; VandeVondele, J.; Rybkin, V. V. Dynamics of the Bulk Hydrated Electron from Many-Body Wave-Function Theory. *Angew. Chem., Int. Ed.* **2019**, *58*, 3890−3893.
(46) Grimme, S.; Antony, J.; Ehrlich, S.; Krieg, H. A consistent and accurate ab initio parametrization of density functional dispersion correction (DFT-D) for the 94 elements H-Pu. *J. Chem. Phys.* **2010**, *132*, 154104.
(47) Guidon, M.; Hutter, J.; VandeVondele, J. Auxiliary Density Matrix Methods for Hartree-Fock Exchange Calculations. *J. Chem. Theory Comput.* **2010**, *6*, 2348−2364.
(48) Humphrey, W.; Dalke, A.; Schulten, K. VMD: Visual molecular dynamics. *J. Mol. Graphics* **1996**, *14*, 33−38.
(49) Smith, P.; Ziolek, R. M.; Gazzarrini, E.; Owen, D. M.; Lorenz, C. D. On the interaction of hyaluronic acid with synovial fluid lipid membranes. *Phys. Chem. Chem. Phys.* **2019**, *21*, 9845−9857.
(50) Wolfram Research, Inc. *Mathematica, Version 13.1*; Wolfram Research, Inc: Champaign, IL, 2024.
(51) Chen, M.; Zheng, L.; Santra, B.; Ko, H.-Y.; DiStasio Jr, R. A.; Klein, M. L.; Car, R.; Wu, X. Hydroxide diffuses slower than hydronium in water because its solvated structure inhibits correlated proton transfer. *Nat. Chem.* **2018**, *10*, 413−419.
(52) Narvaez, W. A.; Wu, E. C.; Park, S. J.; Gomez, M.; Schwartz, B. J. Trap-Seeking or Trap-Digging? Photoinjection of Hydrated Electrons into Aqueous NaCl Solutions. *J. Phys. Chem. Lett.* **2022**, *13*, 8653−8659.
(53) De Grotthuss, C. *Mémoire sur la décomposition de l'eau: et des corps qu'elle tient en dissolution à l'aide de l'électricité galvanique*, 1805.
(54) Bartels, D. M.; Craw, M. T.; Han, P.; Trifunac, A. D. Hydrogen/deuterium isotope effects in water radiolysis. 1. The mechanism of chemically induced dynamic electron polarization generation in spurs. *J. Phys. Chem.* **1989**, *93*, 2412−2421.
(55) Han, P.; Bartels, D. M. Hydrogen/deuterium isotope effects in water radiolysis. 2. Dissociation of electronically excited water. *J. Phys. Chem.* **1990**, *94*, 5824−5833.
(56) Han, P.; Bartels, D. M. Hydrogen/deuterium isotope effects in water radiolysis. 3. Atomic hydrogen in acidic water/water-d2 mixtures. *J. Phys. Chem.* **1991**, *95*, 9370−9374.
(57) Tempra, C.; Chamorro, V. C.; Jungwirth, P. Effects of Water Deuteration on Thermodynamic and Structural Properties of Proteins and Biomembranes. *J. Phys. Chem. B* **2023**, *127*, 1138−1143.
(58) Ceriotti, M.; Fang, W.; Kusalik, P. G.; McKenzie, R. H.; Michaelides, A.; Morales, M. A.; Markland, T. E. Nuclear Quantum Effects in Water and Aqueous Systems: Experiment, Theory, and Current Challenges. *Chem. Rev.* **2016**, *116*, 7529−7550.
(59) Eaves, J. D.; Loparo, J. J.; Fecko, C. J.; Roberts, S. T.; Tokmakoff, A.; Geissler, P. L. Hydrogen bonds in liquid water are broken only fleetingly. *Proc. Natl. Acad. Sci. U.S.A.* **2005**, *102*, 13019−13022.
(60) Bischoff, T.; Reshetnyak, I.; Pasquarello, A. Band gaps of liquid water and hexagonal ice through advanced electronic-structure calculations. *Phys. Rev. Res.* **2021**, *3*, 023182.
(61) Ambrosio, F.; Miceli, G.; Pasquarello, A. Redox levels in aqueous solution: Effect of van der Waals interactions and hybrid functionals. *J. Chem. Phys.* **2015**, *143*, 244508.

https://doi.org/10.1021/acs.jctc.4c00780
J. Chem. Theory Comput. 2024, 20, 7337−7346